ORIGINAL RESEARCH

Dwarf Open Reading Frame (DWORF) Gene Therapy Ameliorated Duchenne Muscular Dystrophy Cardiomyopathy in Aged mdx Mice

Emily D. Morales ⓘ, PhD; Yongping Yue ⓘ, BA; Thais B. Watkins, PhD; Jin Han, BS; Xiufang Pan ⓘ, PhD; Aaron M. Gibson, BS; Bryan Hu, BS; Omar Brito-Estrada ⓘ, BS; Gang Yao, PhD; Catherine A. Makarewich ⓘ, PhD; Gopal J. Babu ⓘ, PhD; Dongsheng Duan ⓘ, PhD

BACKGROUND: Cardiomyopathy is a leading health threat in Duchenne muscular dystrophy (DMD). Cytosolic calcium upregulation is implicated in DMD cardiomyopathy. Calcium is primarily removed from the cytosol by the sarcoendoplasmic reticulum calcium ATPase (SERCA). SERCA activity is reduced in DMD. Improving SERCA function may treat DMD cardiomyopathy. Dwarf open reading frame (DWORF) is a recently discovered positive regulator for SERCA, hence, a potential therapeutic target.

METHODS AND RESULTS: To study DWORF's involvement in DMD cardiomyopathy, we quantified DWORF expression in the heart of wild-type mice and the mdx model of DMD. To test DWORF gene therapy, we engineered and characterized an adeno-associated virus serotype 9–DWORF vector. To determine if this vector can mitigate DMD cardiomyopathy, we delivered it to 6-week-old mdx mice (6×10^{12} vector genome particles/mouse) via the tail vein. Exercise capacity, heart histology, and cardiac function were examined at 18 months of age. We found DWORF expression was significantly reduced at the transcript and protein levels in mdx mice. Adeno-associated virus serotype 9–DWORF vector significantly enhanced SERCA activity. Systemic adeno-associated virus serotype 9-DWORF therapy reduced myocardial fibrosis and improved treadmill running, electrocardiography, and heart hemodynamics.

CONCLUSIONS: Our data suggest that DWORF deficiency contributes to SERCA dysfunction in mdx mice and that DWORF gene therapy holds promise to treat DMD cardiomyopathy.

Key Words: AAV ■ adeno-associated virus ■ cardiomyopathy ■ DMD ■ Duchenne muscular dystrophy ■ DWORF ■ SERCA2a

Duchenne muscular dystrophy (DMD) is a rare muscle-wasting disease caused by mutations in the dystrophin gene.[1] Dystrophin offers structural support to the muscle cell membrane during contraction and relaxation. When dystrophin is absent, muscles undergo degeneration, resulting in muscle weakness and eventual heart and/or respiratory failure. Restoration of dystrophin expression by genetic editing or gene replacement is being actively pursued to treat DMD. An alternative gene therapy approach is to upregulate cellular genes that may mitigate the pathogenic mechanisms of DMD.

It is well documented that dysregulated intracellular calcium contributes directly to muscle cell death in DMD.[2,3] Calcium dysregulation results in an increased concentration of cytosolic calcium, which activates calcium-dependent proteases and phospholipases that digest cellular proteins and lipids, respectively,[4–6]

CLINICAL PERSPECTIVE

What Is New?

- To our knowledge, this is the first study to evaluate dwarf open reading frame (DWORF) expression in an animal model of Duchenne muscular dystrophy (DMD).
- This is the first proof-of-principle study, to our knowledge, suggesting adeno-associated virus-mediated DWORF overexpression may ameliorate Duchenne cardiomyopathy.

What Are the Clinical Implications?

- DMD is a lethal inherited muscle disease without a cure; cytosolic calcium overload is a critical pathogenic mechanism.
- DWORF is a small peptide that boosts cytosolic calcium removal via enhancing sarcoendoplasmic reticulum calcium ATPase activity; we found DWORF expression is reduced in the mdx model of DMD, and AAV-mediated DWORF overexpression significantly reduced DMD heart disease.
- Our results support further development of DWORF gene therapy for DMD.

Nonstandard Abbreviations and Acronyms

AAV	adeno-associated virus
ddPCR	droplet digital PCR
DMD	Duchenne muscular dystrophy
DWORF	dwarf open reading frame
SERCA	sarcoendoplasmic reticulum calcium ATPase
SR	sarcoplasmic reticulum
vg	vector genome particles
WT	wild-type

and contributes to cell death, fibrosis, and diminished contractile function.[7,8] Therefore, strategies aimed at normalizing cytosolic calcium levels in dystrophic cells are expected to reduce muscle disease in DMD.

A major source of cytosolic calcium is the sarcoplasmic reticulum (SR), which is the major intracellular calcium storage site and plays a central role in the contraction-relaxation cycle.[9] In a healthy muscle cell, contraction is initiated as calcium from the SR is released into the cytosol via the opening of the ryanodine receptor. Once in the cytosol, calcium binds to myofilament proteins to initiate contraction. During relaxation, calcium is pumped back into the SR by the sarcoendoplasmic reticulum calcium ATPase (SERCA), leading to its dissociation from contractile proteins.[10,11]

In DMD, however, calcium release from the SR is increased while calcium reuptake into the SR via SERCA is decreased.[12–15] This contributes to increased resting cytosolic calcium concentrations.

One method of reducing cytosolic calcium overload in dystrophic muscle is to enhance SERCA function. This has previously been achieved by SERCA overexpression or knockdown of sarcolipin, a negative regulator of the SERCA pump.[16–22] These treatments significantly reduced the dystrophic phenotype in various mouse models, suggesting that the restoration of calcium homeostasis via enhancing SERCA activity is a promising approach to treating DMD. The micropeptide dwarf open reading frame (DWORF) is a positive regulator of the SERCA pump.[23] It has been shown that DWORF overexpression potently enhances SERCA activity and ameliorates ischemic heart failure and muscle-specific Lin-11, Isl-1, and Mec-3 protein deficiency cardiomyopathy.[24,25] We hypothesize that adeno-associated virus (AAV)-mediated DWORF expression can improve SERCA function and mitigate DMD cardiomyopathy.

To test our hypothesis, we quantified DWORF expression in the hearts of normal and dystrophin-null mdx mice. We found DWORF expression was significantly decreased in mdx mice. We then delivered a DWORF expression cassette with AAV serotype 9 (AAV9) to 6-week-old mdx mice via tail vein injection. DWORF expression, calcium uptake, myocardial fibrosis, electrocardiography, uphill treadmill running, and left ventricular hemodynamics were examined at 18 months of age. In support of our hypothesis, AAV9-mediated DWORF gene transfer significantly enhanced cardiac SR calcium uptake, ameliorated pathological heart remodeling, and improved cardiac function. Our results support further development of DWORF gene therapy to treat DMD cardiomyopathy.

METHODS

The data that support the findings of this study are available from the corresponding author upon reasonable request.

Mice

All animal experiments were approved by the animal care and use committee of the University of Missouri. All mice were maintained in a specific pathogen-free animal care facility on a 12-hour light (25 lux):12-hour dark cycle with access to food and water ad libitum. Dystrophin-deficient mdx mice (C57BL/10ScSn-*Dmd^mdx*/J, stock number 001801) and normal control BL10 (wild-type [WT]; C57BL/10ScSnJ, stock number 000476) mice were originally purchased from The Jackson Laboratory (Bar Harbor, ME). Experimental

mice were generated in-house in a barrier facility using breeders purchased from The Jackson Laboratory. Female mice were used in the current study for the following reasons. First, although DMD is an X-linked disease, females can be afflicted if the mutation occurs in both alleles. Importantly, female patients display a characteristic DMD phenotype.[26] Second, while male mdx mice show more severe skeletal muscle disease, female mdx mice show more severe heart disease.[27,28] The classic presentation of DMD cardiac disease is dilated cardiomyopathy. This is observed in female, but not male, mdx mice.[27,29] The sample size shown in the figures refers to the number of mice used in the assay.

AAV Production and Administration

The *cis*-plasmid for AAV packaging (also called pEM1) consisted of (from 5′-end to 3′-end) the ubiquitous cytomegalovirus immediate-early enhancer/chicken β-actin promoter, a codon-optimized mouse DWORF cDNA, the encephalomyocarditis virus internal ribosomal entry site (Clontech, Mountain View, CA), the EGFP (enhanced green fluorescence protein) gene, and an SV40 virus polyadenylation signal. The codon-optimized mouse DWORF cDNA was synthesized by GenScript (Piscataway, NJ). The vector genome was packaged in the capsid of AAV9 and purified through 2 rounds of isopycnic ultracentrifugation according to our previously published method.[30] AAV was delivered to 6-week-old mice via tail vein injection at a concentration of 6×10^{12} vector genome particles (vg)/mouse.

Western Blot

For DWORF western blots, freshly isolated heart and soleus tissues were snap-frozen in liquid nitrogen and homogenized in radioimmunoprecipitation assay buffer (150 mmol/L NaCl; 1% v/v IGEPAL CA-630; 50 mmol/L Tris-Cl, pH 8.0; 0.1% w/v sodium deoxycholate; 0.1% w/v sodium dodecyl sulfate) with added protease inhibitors (cOmplete ULTRA mini-tablet, Roche, Indianapolis, IN); 40 µg of the heart lysate was run on 15% bis/acrylamide gels made by standard preparation, and proteins were transferred to polyvinylidene fluoride membranes membranes (Millipore, Immoblion-P) by wet transfer technique. Membranes were incubated with a previously validated custom rabbit polyclonal antibody against mouse DWORF (New England Peptide) at a concentration of 1:1000.[23] Blots were incubated with a goat anti-rabbit immunoglobulin G horseradish peroxidase secondary antibody and developed using ClarityTM Western ECL chemiluminescent substrate (Bio-Rad, Hercules, CA) and a digital Bio-Rad ChemiDocTM MP Imaging System.

For all other western blots, tissues were homogenized in lysis buffer (50 mmol/L Tris, pH 7.4, 150 mmol/L NaCl, 1 mmol/L EDTA, and 0.5% NP-40)

with added 1 mmole phenylmethylsulfonyl fluoride, 5 mmole sodium metavanadate, 10 nmole okadaic acid, 1 mmole sodium fluoride, and 1 mmole benzamidine. Heart lysates were run on sodium dodecyl sulfate-polyacrylamide gels. Proteins were then electroblotted onto polyvinylidene fluoride membranes and incubated with antibodies specific for sarcolipin (anti-rabbit, 1:3000),[31] SERCA2a (anti-rabbit, 1:5000, custom made),[31] phospholamban (anti-rabbit, 1:3000, custom made),[31] calsequestrin (anti-rabbit, 1:5000, Affinity BioReagents, Golden, CO), or GAPDH (anti-mouse, 1:10000, Sigma, St. Louis, MO). Quantification was completed using ImageJ/Fiji Software (ImageJ 1.48b) and then normalized to GAPDH levels.

Endogenous DWORF Transcript Quantification

Endogenous DWORF transcript was quantified using droplet digital PCR (ddPCR) methods with the primers and probe as previously described.[23] Specifically, primer and probe sets were designed as follows: Forward primer: 5′-TTCTTCTCCTGGTTGGATGG-3′, Reverse primer: 5′- TCTTCTAAATGGTGTCAGAT TGAAGT-3′, and Probe 5′- TTTACATTGTCTTCTTC TAGAAAAGGAAGAAG-3′. Probes were labeled with a 5′ 6-carboxyfluorescein, an internal ZEN quencher, and a 3′ Iowa Black quencher. Tissue samples were collected and stored in RNAlater stabilization solution (Thermo Fisher Scientific, Waltham, MA; Cat No: AM7021) until RNA was extracted using the RNeasy Fibrous Tissue Mini kit (Qiagen, Hilden, Germany; Cat No: 74704). Reverse transcription was performed using the SuperScript IV VILO Master Mix with ezDNase Enzyme (Thermo Fisher Scientific, Cat No: 11766050), and the resulting cDNA concentrations were detected using the Qubit ssDNA assay kit (Thermo Fisher Scientific, Cat No: Q10212). The ddPCR was completed on the QX200 ddPCR system (Bio-Rad) using ddPCR supermix for probes (no dUTP) (Bio-Rad, Cat No: 186–3024). Results were presented as the number of transcript copies per ng of cDNA used in the ddPCR reaction.

SR Calcium Uptake

SR calcium uptake was measured using a previously described Millipore filtration technique.[20] Approximately 150 µg of ventricular protein extract was incubated at 37 °C in 1.5 mL of calcium uptake medium (40 mmol/L imidazole, pH 7.0, 100 mmol/L KCl, 5 mmol/L $MgCl_2$, 5 mmol/L NaN_3, 5 mmol/L potassium oxalate, 0.5 mmol/L EGTA), and various concentrations of $CaCl_2$ to yield 0.03–3 µmol/L free calcium. Ruthenium red was added to a final concentration of 1 µmole immediately before adding substrates to begin calcium uptake. A final concentration of 5 mmole ATP was added to initiate

the reaction. The reaction was terminated at 1 minute by filtration. The rate of SR calcium uptake and the calcium concentration required for EC50 were determined by nonlinear curve fitting analysis using GraphPad Prism v6.01 software (GraphPad, San Diego, CA).

ECG and Hemodynamic Assay

Twelve-lead ECG was performed using a commercial system from AD Instruments (Colorado Springs, CO, USA). Results were evaluated using our previously published standard operating protocol in "Cardiac protocols for Duchenne animal models" (http://www.parentprojectmd.org/site/PageServer?pagename=Advance_researchers_sops).[32] All ECG parameters but Q wave amplitude were analyzed using the lead II tracing. Q wave amplitude was determined using the lead I tracing. QTc interval was calculated by correcting the QT interval with the heart rate as described by Mitchell et al.[33] The cardiomyopathy index was calculated by dividing the QT interval by the PQ segment.[34] Left ventricular hemodynamics was performed using our previously described closed chest approach with the Millar catheter, which can also be found in the "Cardiac protocols for Duchenne animal models".[32] The resulting pressure-volume loops were analyzed using the PVAN software (Millar Instruments, Houston, TX, USA). Cardiac relaxation time constant (Tau) was calculated according to Weiss et al.[35] Body surface area was calculated as described by Cheung et al.[36]

Treadmill Running

The treadmill endurance assay was performed according to previous protocols but with minor modifications.[19,29] Mice were subjected to 5 days of treadmill acclimation and training on a 7° uphill treadmill (Columbus Instruments, Columbus, OH, USA). During training, mice were encouraged to run by gently nudging mice from behind with a ruler. Each training day began with acclimating mice to a flat, unmoving treadmill surface for 2 minutes. The rest of the protocol was conducted at a 7° incline. Training days were conducted as follows: (Day 1) mice acclimated to an unmoving treadmill surface for 5 minutes, mice ran for 15 minutes at 5 m/min, mice ran for 5 minutes at 10 m/min; (Day 2) mice ran for 5 minutes at 5 m/min, mice ran for 15 minutes at 10 m/min, mice ran for 5 min at 12 m/min; (Day 3) mice ran for 5 minutes at 5 m/min, mice ran for 15 minutes at 10 m/min, mice ran for 10 min at 12 m/min; (Day 4) mice ran for 5 minutes at 5 m/min, mice ran for 20 minutes at 10 m/min, mice ran for 5 min at 12 m/min, mice ran for 5 minutes at 15 m/min; and (Day 5) mice ran for 5 minutes at 5 m/min, mice ran for 20 minutes at 10 m/min, mice ran for 5 min at 12 m/min, mice ran for 5 minutes at 15 m/min. On day 6, mice were again acclimated to a flat, unmoving treadmill surface for 2 minutes. Then, mice ran at a 7° incline for 5 minutes at 5 m/min. The speed of running was then increased by 1 m/min every 5 minutes until mice were exhausted. Exhaustion was diagnosed when a mouse exited the treadmill and refused to reenter, despite gentle nudging, for 3 seconds. At this point, total running distance was recorded. Results were recorded as distance run/mouse body weight.

Morphological Studies

A total of 10 μm cryosections were sectioned from optimal cutting temperature-embedded heart samples. General histology was examined by hematoxylin and eosin staining. Fibrosis was examined by Masson trichrome staining, which was conducted using the Masson Trichrome Stain Kit (Epredia, Kalamazoo, MI). To quantify the percent of the fibrotic area, a transverse section in the middle of the heart was stained with Masson trichrome. The blue-stained fibrotic area in the entire heart section was quantified using ImageJ/Fiji Software (ImageJ 1.48b). The sum of all fibrotic areas was then represented as a percentage of the whole cross-sectional area.

Statistical Analysis

Data are presented as mean±SEM. Statistical analysis was performed using the Statistics and Machine Learning Toolbox (https://www.mathworks.com/products/statistics.html; V12.3; Matlab 2022a, Mathworks Inc., Natick, MA). The Anderson-Darling test was used to determine data distribution. The 2-group comparison data (except for western blot quantification of DWORF expression in untreated mdx and AAV-treated mdx mice) showed normal distribution. The statistical significance of these comparisons was determined by the Student's t test. Most 3-group comparison data (wild-type, mdx, and AAV-treated mdx) showed normal distribution. The statistical significance of these data was determined by 1-way ANOVA with the Tukey–Kramer test for post hoc pairwise comparison. Non-normal distribution was found in a subset of 3-group comparison data. These data were analyzed with the nonparametric Kruskal–Wallis test. A $P<0.05$ was considered statistically significant.

RESULTS

DWORF Expression Was Decreased in the Hearts of mdx Mice

Previous studies suggest SERCA function is reduced in DMD.[12,15,19,20] To determine whether DWORF plays a role, we compared DWORF cDNA and protein levels in the ventricles of 6-month-old mdx and wild-type BL10 (WT) mice (Figure 1). Compared with WT hearts, DWORF cDNA levels were significantly decreased in mdx hearts as assessed by ddPCR (Figure 1A). Consistent with the cDNA data, western blot analysis
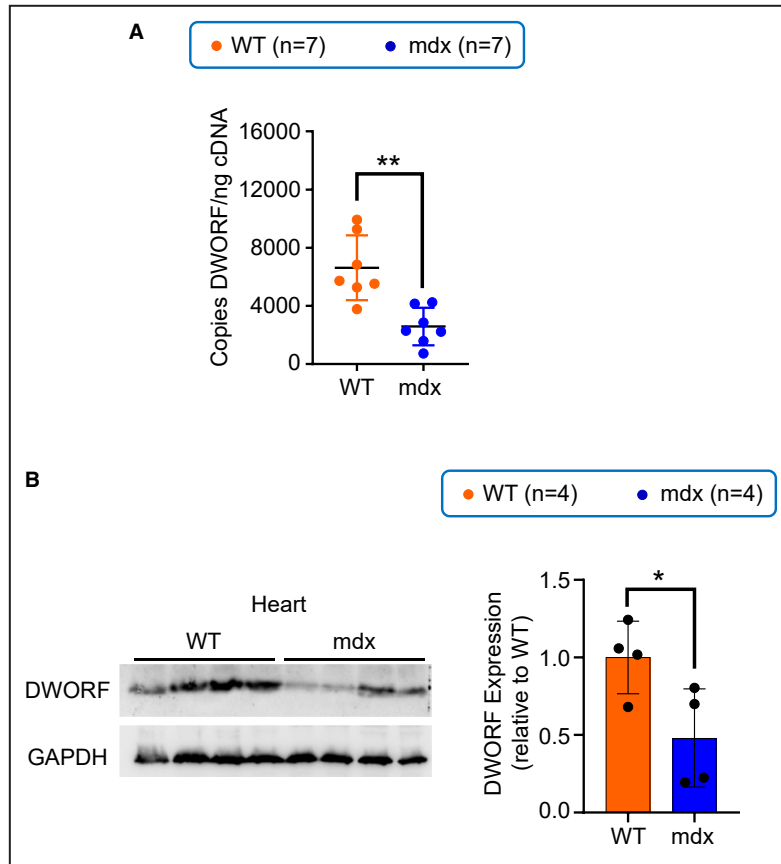
Figure 1.   Dwarf open reading frame (DWORF) expression was decreased in mdx mouse hearts.
A, Quantification of DWORF transcript in the ventricle of 6-month-old wild-type BL10 and mdx mice. **B**, Quantification of DWORF protein expression in the ventricles of 6-month-old wild-type and mdx mice by western blot. The left panel shows western blot images, and the right panel shows densitometry results. Sample size refers to the number of mice used in the study. DWORF indicates Dwarf open reading frame; and WT, wild-type. * $P<0.05$; **$P<0.01$.

showed an ≈50% decrease in DWORF protein expression in the mdx ventricle compared with the WT ventricle (Figure 1B; Figure S1A). Additional studies suggest that DWORF expression was also significantly reduced in the ventricles of 6-week-old and 18-month-old mdx mice (Figure S2).

AAV-DWORF Delivery Increased DWORF Expression and Enhanced SR Calcium Uptake in the mdx Mouse Heart

To develop a DWORF gene therapy approach, we engineered an AAV9-DWORF vector (Figure 2A). In this vector, a codon-optimized mouse DWORF cDNA was expressed from the ubiquitous cytomegalovirus immediate-early enhancer/chicken β-actin promoter. To facilitate the detection of AAV transduction, we also introduced the EGFP cDNA under the control of an internal ribosomal entry site. The AAV genome was packaged in myocardial-tropic AAV9 capsids.[37] We

injected the AAV9-DWORF vector to 6-week-old mdx mice at the dose of 6×10^12 vg/mouse via the tail vein and examined DWORF expression in the ventricle when mice reached 6 months of age (Figure 2B; Figure S1B). Supraphysiological levels of DWORF expression were detected in the AAV-injected mdx mouse hearts (≈50-fold higher than those of uninjected mdx mouse hearts). For reasons yet unknown, we failed to detect EGFP expression (Figure S3). Despite the dramatic increase of DWORF expression in AAV-injected mdx mice, no significant changes were detected in the transcript level of the endogenous DWORF gene (Figure S4), nor were protein levels of SERCA2a (SERCA isoform expressed in the heart), calsequestrin, sarcolipin, or phospholamban altered (Figure 2C; Figure S1C).

Next, we analyzed SR calcium uptake in the ventricular extracts (Figure 2D and 2E). As expected, SR calcium uptake was reduced in mdx hearts compared with WT controls. AAV9-DWORF delivery significantly enhanced SR calcium uptake in the mdx heart (Figure 2D). The
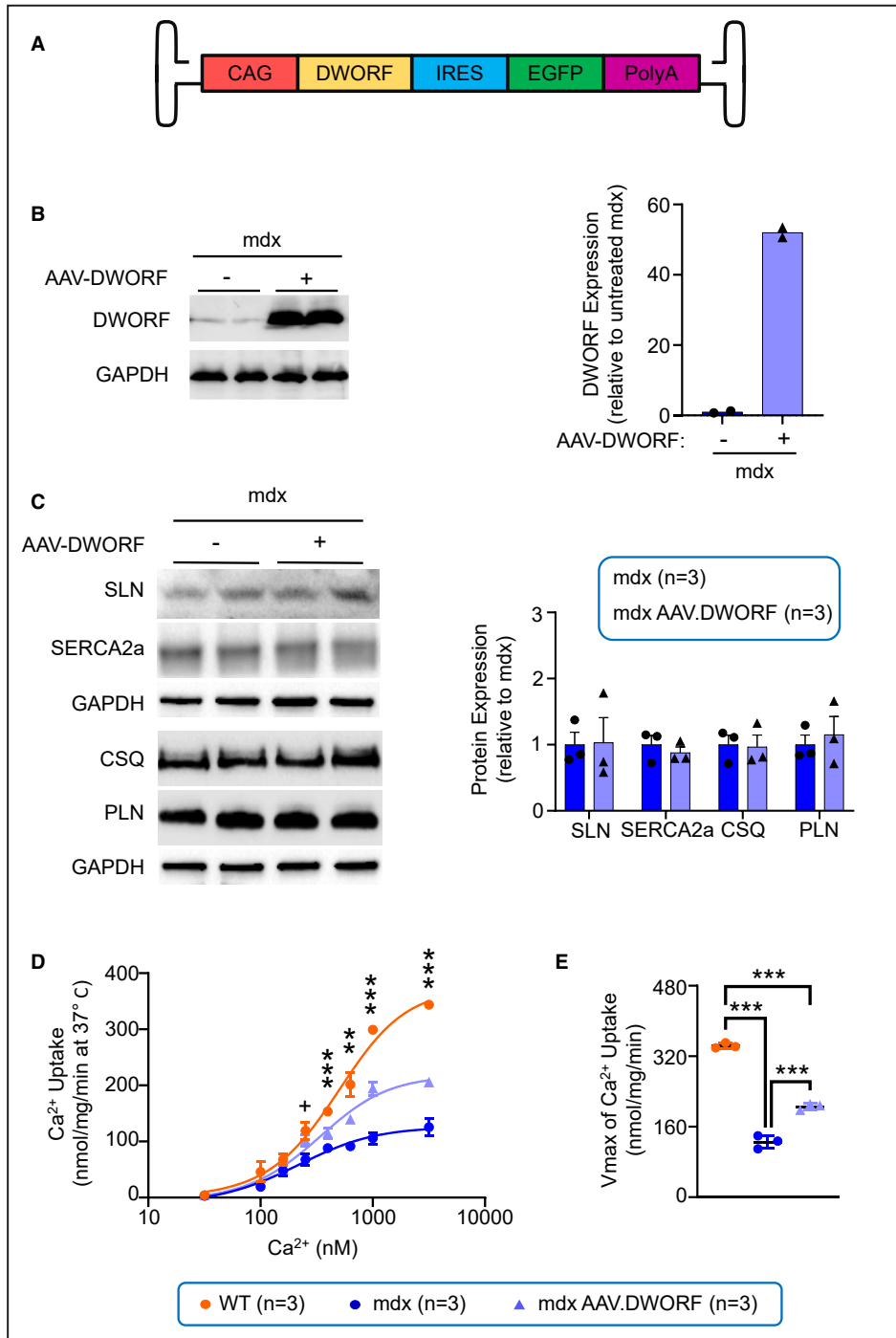
maximum velocity of calcium uptake was also significantly increased (Figure 2E). Nonetheless, improvements did not reach the levels of WT mouse hearts.

AAV-DWORF Delivery Did Not Change Heart Mass But Reduced Myocardial Fibrosis in Aged mdx Mice

After validation of the AAV9-DWORF vector, we evaluated its therapeutic effects in mdx mice (6×10^{12} vg/mouse, tail vein injection at 6 weeks of age, examination at 18 months of age). We opted to study 18-month-old mice because this is the age at which mdx mice display dilated cardiomyopathy.[38] On anatomic examination, we did not detect significant differences in the heart weight, ventricular weight, and weight ratios between DWORF-treated and saline-injected control mdx mice (Table). On histological examination, we performed Masson trichrome staining and quantified fibrosis (Figure 3). DWORF gene therapy significantly reduced myocardial fibrosis compared with saline-injected mdx mice.

Figure 2. Adeno-associated virus–Dwarf open reading frame (AAV-DWORF) delivery at 6 weeks of age increased DWORF expression and sarcoendoplasmic reticulum calcium uptake in mdx hearts at 18 months of age.

A, Schematic drawing of the adeno-associated virus–DWORF vector. **B**, Quantification of DWORF protein expression in the ventricles by western blot. The left panel shows western blot images, and the right panel shows densitometry results. **C**, Quantification of the expression of various calcium-handling proteins in the ventricles. The left panel shows representative western blot images, and the right panel shows densitometry results. Please note sarcoendoplasmic reticulum calcium ATPase 2a and sarcolipin blots were run with 1 set of lysates, while calsequestrin and phospholamban were run with another. **D**, Heart sarcoendoplasmic reticulum calcium-dependent calcium uptake curve. **E**, Maximum rate of calcium uptake in the heart. Sample size refers to the number of mice used in the study. AAV, adeno-associated virus; CAG, cytomegalovirus immediate-early enhancer/chicken β-actin promoter; DWORF, dwarf open reading frame; EGFP, enhanced green fluorescence protein; IRES, internal ribosome entry site; polyA, polyadenylation signal; SERCA2a, sarcoendoplasmic reticulum calcium ATPase type 2a; and WT, wild-type. **$P<0.01$ between all compared groups, ***$P<0.001$ between all compared groups, +$P<0.05$ between mdx and all other groups, but there is no statistically significant difference between wild-type BL10 and adeno-associated virus–Dwarf open reading frame-treated mdx mice.

AAV-DWORF Delivery Ameliorated mdx ECG Defects

To determine whether DWORF gene therapy can improve cardiac electrophysiology, we performed ECG (Figure 4; Figure S5). All parameters showed expected changes in mdx mice compared with WT mice (Figure 4; Figure S5). DWORF therapy normalized the heart rate, QTc interval, and cardiomyopathic index in mdx mice. Other ECG parameters (PR interval, QRS duration, and Q amplitude) showed a trend of improvement but was not statistically significant.

AAV-DWORF Delivery Improved Uphill Treadmill Running

Uphill treadmill running is frequently used to evaluate mouse heart function.[19,29,39] Following 5 days of acclimation, we quantified mouse running distance on a 7° uphill treadmill. Mdx mice ran an average of 82 m or 3.3 m/g body weight (m/g). WT mice ran an average of 603 m or 20.9 m/g (Figure 5). DWORF gene therapy increased treadmill performance ($P=0.065$).

Table. Weights and Weight Ratios at 18 Months of Age (mean±SEM)

	Wild-type	mdx	mdx AAV-DWORF
Sample size, n	15	14	11
BW, g	28.24±0.52	22.95±0.37*	22.67±0.65*
HW, mg	98.87±1.95	104.45±2.15	104.60±3.61
VW, mg	94.11±2.00	100.59±2.08	101.18±3.44
TL, mm	18.17±0.06	18.72±0.07*	18.57±0.09*
TW, mg	33.07±0.75	28.69±1.04*	27.29±1.01*
HW/BW, mg/g	3.52±0.09	4.56±0.10*	4.61±0.09*
HW/ TL, mg/mm	5.44±0.11	5.58±0.12	5.63±0.18
TW/BW, mg/mg	1.18±0.04	1.25±0.04	1.20±0.03
HW/TW, mg/mg	3.00±0.06	3.69±0.13*	3.85±0.0.10*
VW/BW, mg/g	3.35±0.08	4.39±0.09*	4.46±0.09*
VW/TL, mg/mm	5.18±0.11	5.38±0.12	5.44±0.17
VW/TW, mg/mg	2.86±0.05	3.56±0.12*	3.73±0.10*

BW indicates body weight; HW, heart weight; TL, tibia length; TW, tibialis anterior muscle weight; and VW, ventricle weight.

*Significantly different from wild-type.

Treated mice reached an average of 198 m or 8.0 m/g (Figure 5).

AAV-DWORF Delivery Enhanced Left Ventricular Hemodynamic Function in mdx Mice

Cardiac pump function was evaluated using a closed-chest catheterization assay as we previously reported.[34] Consistent with our previous publications,[19,27,38] saline-injected mdx mice showed a classic profile of dilated cardiomyopathy (Figure 6; Table S1; Figures S6 and S7). Specifically, end-systolic and end-diastolic chamber volumes were significantly enlarged, while the ejection fraction, maximum pressure, and rates of pressure change during contraction (dP/dt max) and relaxation (dP/dt min) were significantly decreased. DWORF gene therapy normalized maximum pressure and ejection fraction in mdx mice. A trend of improvement was also detected in dP/dt max and dP/dt min. Intriguingly, end-systolic and end-diastolic volumes of the AAV9-DWORF-treated mdx mice were smaller than those of WT mice, although statistical significance between WT mice and DWORF-treated mdx mice was only observed for the end-diastolic volume. The only parameter that showed no improvement was tau, the time constant of left ventricular relaxation.

DISCUSSION

In this study, we evaluated DWORF expression levels in normal and dystrophic mouse hearts and explored AAV-DWORF gene therapy for Duchenne cardiomyopathy in the mdx mouse model of DMD. We found that endogenous DWORF expression was significantly reduced at both the transcript and protein levels in mdx hearts (Figure 1; Figures S1A and S2). Intravenous delivery of an AAV9-DWORF vector resulted in supraphysiological levels of DWORF expression in the mdx heart and significantly improved cardiac SR calcium uptake (Figure 2; Figure S1B). Importantly, a single dose of AAV-DWORF gene therapy in 6-week-old mdx mice resulted in significant improvements in myocardial
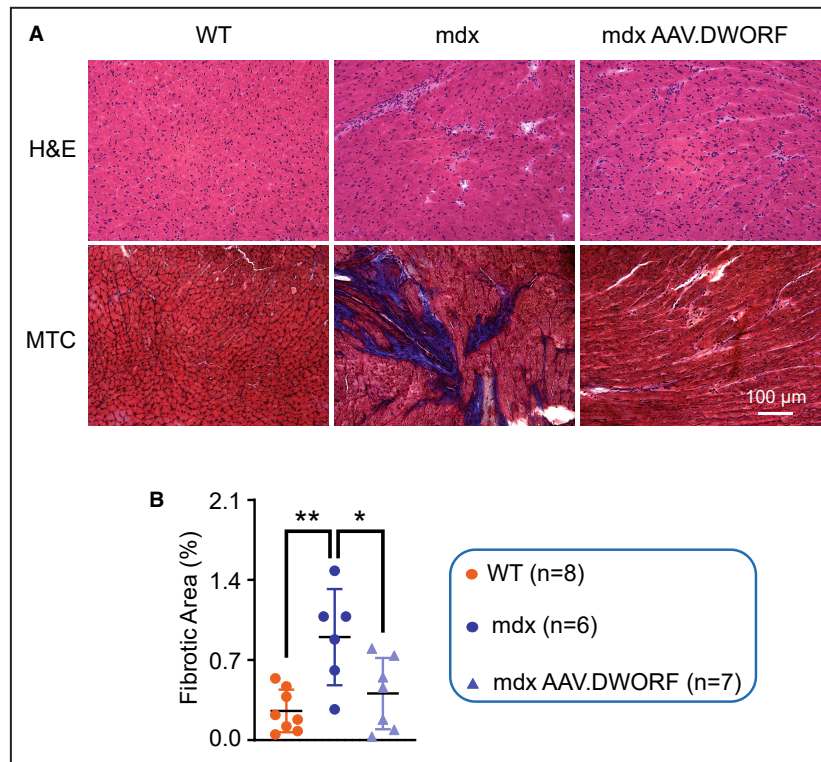
Figure 3. Adeno-associated virus–Dwarf open reading frame (AAV-DWORF) delivery at 6 weeks of age ameliorated fibrosis in treated mdx mice at 18 months of age.
A, Representative photomicrographs of hematoxylin and eosin and Masson trichrome staining from wild-type BL10, saline-injected mdx, and adeno-associated virus–DWORF-treated mdx mouse ventricles. **B**, Quantification of the fibrotic area in the ventricles. Sample size refers to the number of mice used in the study. AAV indicates adeno-associated virus; DWORF, dwarf open reading frame; H&E, hematoxylin and eosin; MTC, Masson Trichrome; and WT, wild-type. *$P<0.05$; **$P<0.01$.

histology, uphill running, ECG, and left ventricular hemodynamics at 18 months of age (Figures 3 through 6, Table S1, Figures S5 through S7). Our results suggest (1) decreased DWORF expression may contribute to SERCA dysfunction in dystrophic cardiac tissue and (2) DWORF gene therapy at a young age holds promise to significantly prevent dilated cardiomyopathy in DMD.

DWORF was discovered in 2016 as a small peptide encoded in a long noncoding RNA.[23] It is the only known endogenous SERCA activator. DWORF is exclusively expressed in ventricular and slow-twitch skeletal muscle fibers. Initial studies suggest DWORF enhances SERCA function through competition with inhibitory peptides sarcolipin and phospholamban for SERCA binding.[23,24,40] More recent studies suggest DWORF may also directly activate SERCA.[41,42] It is possible both mechanisms are in play.[43] More studies are needed to clarify this.

Recently, DWORF has received attention for playing a large role in the development and treatment of cardiomyopathy. DWORF expression was reduced in 2 independent mouse models of heart failure, including myocardial infarction and a genetic model of dilated cardiomyopathy caused by the loss of the muscle-specific Lin-11, Isl-1, and Mec-3 protein.[24,25] Expression of DWORF via a transgenic approach or AAV9-DWORF gene delivery enhanced SERCA activity, ameliorated pathological cardiac remodeling, and improved heart function in these models.[24,25]

It is well established that decreased SERCA activity contributes to DMD pathogenesis.[2,3,8] Previous studies have connected SERCA dysfunction with sarcolipin overexpression.[15,20,44] Indeed, sarcolipin knockdown ameliorated dystrophic phenotypes in murine DMD models.[20–22] The discovery of DWORF as a positive SERCA regulator raises the possibility of DWORF downregulation as a contributing mechanism for SERCA activity reduction in DMD. Given the established involvement of DWORF in other types of cardiomyopathies, we focused the current study on DMD heart disease.

In the mouse myocardial infarction model, DWORF expression was reduced by ≈60%.[25] In the muscle-specific Lin-11, Isl-1, and Mec-3 protein-deficient
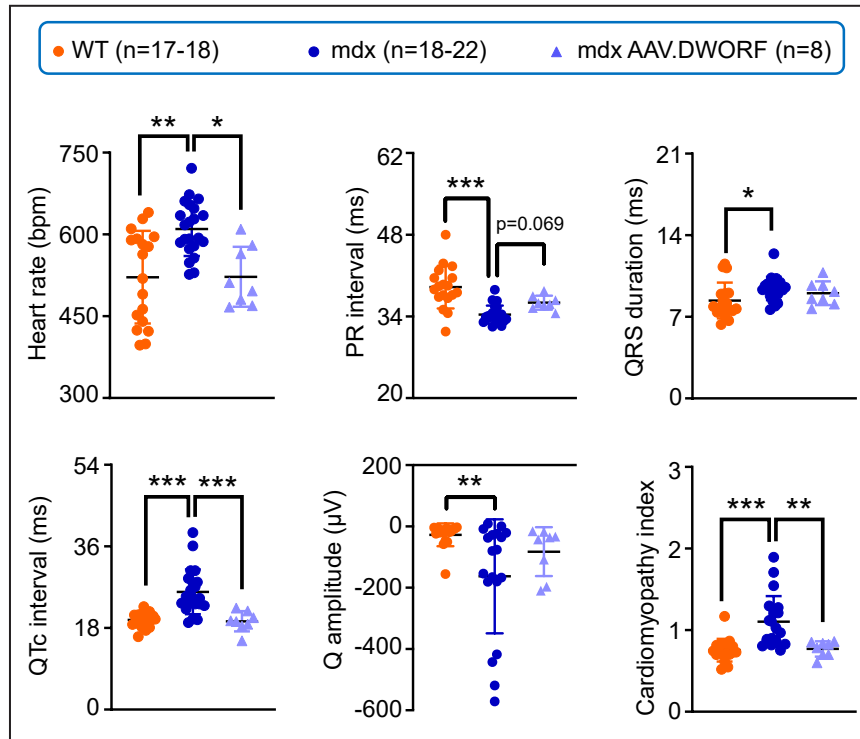
Figure 4. Adeno-associated virus–Dwarf open reading frame (AAV-DWORF) delivery at 6 weeks of age improved ECG at 18 months of age.
ECG evaluation of heart rate, PR interval, QRS duration, QTc interval, Q amplitude, and cardiomyopathy index. Sample size refers to the number of mice used in the study. AAV indicates adeno-associated virus; DWORF, dwarf open reading frame; and WT, wild-type. *$P < 0.05$; **$P < 0.01$; ***$P < 0.001$. Results from the heart rate, PR interval, QRS duration, Q amplitude, and cardiomyopathy index were analyzed by the Kruskal–Wallis test. Box plot (median, 25% and 75% interquartile range) presentations of these data are shown in Figure S5.

cardiomyopathy model, DWORF expression was reduced by ≈70%.[24] Consistent with these results, we found DWORF expression was reduced by ≈50% in the mdx heart (Figure 1; Figure S1A). These results suggest low-level DWORF expression (30%–50% of the WT level) is likely insufficient for normal SERCA function.

To establish a causal relationship between DWORF downregulation and SERCA dysfunction, we delivered an AAV9-DWORF vector (6×10^{12} vg/mouse) to the heart of mdx mice via tail vein injection. Compared with saline-injected mdx hearts, AAV-injected mdx hearts exhibited an approximately 50-fold increase in DWORF levels (Figure 2B; Figure S1B). This is ≈25-fold higher than that of WT hearts. Despite supraphysiological DWORF expression, myocardial SR calcium uptake was only partially restored (Figure 2D and 2E). This suggests DWORF downregulation may have contributed to SERCA activity reduction in the mdx heart, but it is unlikely the sole cause. Previous literature shows DWORF has a higher SERCA binding affinity than phospholamban,[23,24] but there is no literature covering

the dynamics of DWORF versus sarcolipin competition in the heart. It has been shown that sarcolipin expression is elevated in the heart of mdx mice.[20] DWORF overexpression has no effect on sarcolipin expression in mdx ventricles (Figure 2C). Therefore, it is possible that sarcolipin will strongly compete with DWORF for binding to SERCA, thereby limiting SERCA activation by ectopic DWORF. Alternatively, there may exist additional yet unknown SERCA inhibition mechanism(s) in the mdx heart that cannot be revoked by DWORF overexpression.

We also examined the expression of several other SR calcium-regulating proteins and did not see significant alterations (Figure 2C; Figure S1C). This is consistent with what has been shown in DWORF transgenic mice, where proteins involved in calcium handling are largely unaffected.[23]

To explore DWORF as a potential therapeutic target for Duchenne cardiomyopathy, we followed AAV9-DWORF injected mdx mice until they reached 18 months of age (Figures 3–6). This is necessary because young adult mdx mice display minimal heart disease.[45] On
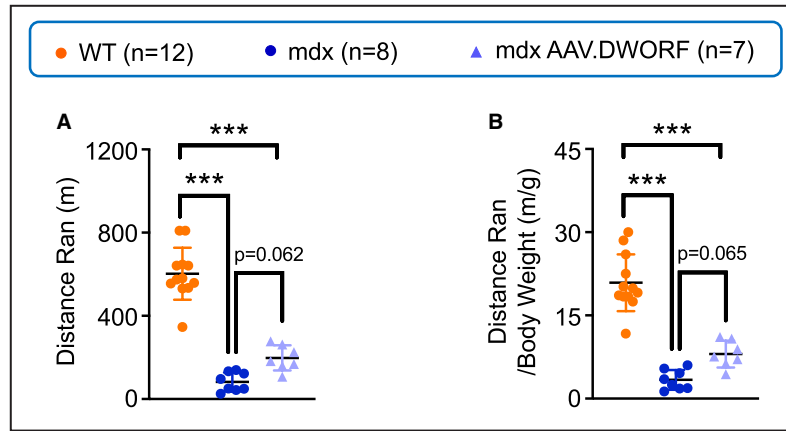
Figure 5. Adeno-associated virus–Dwarf open reading frame (AAV-DWORF) delivery at 6 weeks of age improved uphill treadmill running at 18 months of age.
A, Total distance run on a 7° uphill treadmill. **B**, Total distance run on a 7° uphill treadmill normalized by mouse body weight. Sample size refers to the number of mice used in the study. AAV indicates adeno-associated virus; DWORF, dwarf open reading frame; and WT, wild-type. ***$P<0.001$.

anatomical examination, no statistically significant improvement was detected (Table). Nevertheless, cardiac fibrosis, ECG, closed-chest cardiac catheter assay, and uphill treadmill running showed significant improvements in many, though not all, parameters (Figures 3–6). This is expected given that SR calcium uptake was only partially restored in treated mice (Figure 2D and 2E).

We have previously conducted a similar long-term study in mdx mice using the AAV9.SERCA2a vector.[19] Systemic injection of the same dose (6×10^{12} vg/mouse) of SERCA2a vector completely corrected cardiac SR calcium uptake, prevented myocardial fibrosis, and normalized most parameters in physiology assays (ECG, heart hemodynamics, and uphill treadmill running). The difference in the therapeutic outcome between DWORF and SERCA2a gene therapy suggests that there is room to further improve DWORF gene therapy. This can be accomplished by several approaches. One is to further increase DWORF expression. Makarewich and colleagues found that ≈60-fold DWORF overexpression resulted in better cardioprotection than ≈17-fold DWORF overexpression in a dilated cardiomyopathy mouse model caused by genetic knockout of the gene encoding the muscle-specific Lin-11, Isl-1, and Mec-3 protein.[24,25] We are not in favor of this approach because (a) increasing the AAV dose may lead to severe adverse consequences, even death[46]; and (b) an ex vivo study in isolated rat hearts suggests that exogenous administration of high-dose DWORF peptide may induce coronary vasoconstriction.[47]

Another approach is to combine sarcolipin knockdown and DWORF overexpression. On one hand, SERCA inhibition will be reduced (by lowering sarcolipin expression and/or by enhancing SERCA function through DWORF binding).[41,42] On the other hand, a

potential caveat of this approach is SERCA overactivation. Law et al ablated phospholamban from mdx mice.[48] These mice showed enhanced calcium handling and myocardial contractility, but heart function was worsened, and cardiac fibrosis was aggravated. Similarly, genetic deletion of sarcolipin from mdx mice resulted in more severe skeletal muscle disease.[49] It is possible that enhanced contractility from untuned calcium cycling may have made the dystrophic sarcolemma more fragile, hence causing more damage.

A third approach is to combine DWORF overexpression with microdystrophin gene therapy. Systemic AAV microdystrophin gene therapy is currently being tested in patients with DMD.[50] Microdystrophin reestablishes the linkage between the cytoskeleton and the extracellular matrix to maintain sarcolemmal integrity during contraction. Despite encouraging data in murine models, microdystrophin only resulted in limited force improvement in the canine DMD model.[51] A recent phase II trial also failed to yield significant functional improvements in all patients.[52] Multiple strategies have been proposed to enhance microdystrophin gene therapy. One possibility is to combine microdystrophin with therapies that can improve calcium homeostasis in muscle cells. In this regard, DWORF has a unique advantage. The small size of the DWORF cDNA (102 bp) makes it possible to fit into existing microdystrophin vectors. Future side-by-side comparisons of the microdystrophin vector, the DWORF vector, and the microdystrophin/DWORF vector will show whether the combined approach is indeed superior.

Our study has several limitations. First, a ubiquitous promoter was used in the current study. From the standpoint of gene therapy, future studies should be conducted using muscle-specific promoters to limit
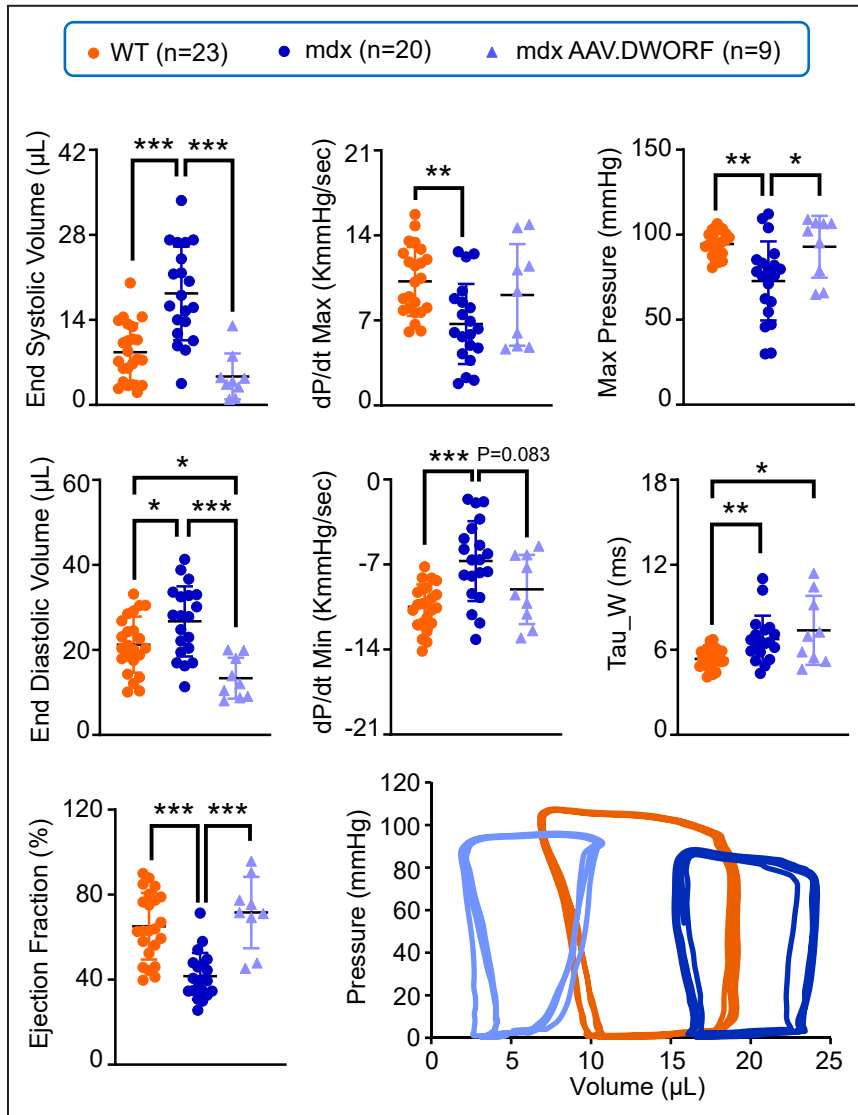
Figure 6. Adeno-associated virus–Dwarf open reading frame (AAV-DWORF) delivery at 6 weeks of age improved left ventricular hemodynamics at 18 months of age.

Evaluation of left ventricular hemodynamics, including the end-systolic volume, end-diastolic volume, maximum pressure, ejection fraction, time constant of left ventricular relaxation (Tau), dP/dt max, and dP/dt min. Representative pressure-volume loops from wild-type BL10, mdx, and adeno-associated virus–Dwarf open reading frame-treated mdx mice (bottom right panel). Sample size refers to the number of mice used in the study. AAV, adeno-associated virus; DWORF, dwarf open reading frame; and WT, wild-type. *$P<0.05$; **$P<0.01$; ***$P<0.001$. Results from the maximum pressure and Tau W were analyzed by the Kruskal–Wallis test. Box plot (median, 25% and 75% interquartile range) presentations of these data are shown in Figure S6.

off-target expression in nonmuscle tissues. Second, we focused our study on mdx mice. Despite significant improvement in multiple electrophysiological and hemodynamic parameters, the left ventricular relaxation time constant Tau, the most established index for left ventricular diastolic function, was not improved. This suggests the existence of diastolic dysfunction in DWORF-treated mdx mice. Future studies in WT mice

will help clarify whether DWORF overexpression may induce diastolic dysfunction. Third, we have focused our study on treating DMD heart disease. Interestingly, we found DWORF expression was also significantly reduced in the soleus muscle of mdx mice (Figure S8). It is likely that systemic AAV-DWORF therapy may also ameliorate dystrophic skeletal muscle disease. In support, the improvement in uphill treadmill running may

be partly attributable to the effect on skeletal muscle (Figure 5). Future studies are needed to thoroughly examine skeletal muscle histology and force in mdx mice that have received systemic AAV DWORF therapy.

In summary, our study demonstrates for the first time, to our knowledge, that DWORF expression was reduced in mdx hearts and AAV-DWORF gene therapy prevented the deterioration of mdx mouse heart function. Future studies will shed light on whether AAV-DWORF therapy can ameliorate dystrophic skeletal muscle disease in mice, and more importantly, whether positive findings seen in our study can be translated to canine models and eventually benefit human patients.

REFERENCES

1. Duan D, Goemans N, Takeda S, Mercuri E, Aartsma-Rus A. Duchenne muscular dystrophy. *Nat Rev Dis Primers*. 2021;7:13. doi: 10.1038/s41572-021-00248-3

2. Burr AR, Molkentin JD. Genetic evidence in the mouse solidifies the calcium hypothesis of myofiber death in muscular dystrophy. *Cell Death Differ*. 2015;22:1402–1412. doi: 10.1038/cdd.2015.65

3. Mareedu S, Million ED, Duan D, Babu GJ. Abnormal calcium handling in Duchenne muscular dystrophy: mechanisms and potential therapies. *Front Physiol*. 2021;12:647010. doi: 10.3389/fphys.2021.647010

4. Hopf FW, Turner PR, Denetclaw WF Jr, Reddy P, Steinhardt RA. A critical evaluation of resting intracellular free calcium regulation in dystrophic mdx muscle. *Am J Physiol*. 1996;271:C1325–C1339. doi: 10.1152/ajpcell.1996.271.4.C1325

5. Turner PR, Westwood T, Regen CM, Steinhardt RA. Increased protein degradation results from elevated free calcium levels found in muscle from mdx mice. *Nature*. 1988;335:735–738. doi: 10.1038/335735a0

6. Lindahl M, Backman E, Henriksson KG, Gorospe JR, Hoffman EP. Phospholipase A2 activity in dystrophinopathies. *Neuromuscul Disord*. 1995;5:193–199. doi: 10.1016/0960-8966(94)00045-B

7. Rahimov F, Kunkel LM. The cell biology of disease: cellular and molecular mechanisms underlying muscular dystrophy. *J Cell Biol*. 2013;201:499–510. doi: 10.1083/jcb.201212142

8. Law ML, Cohen H, Martin AA, Angulski ABB, Metzger JM. Dysregulation of calcium handling in Duchenne muscular dystrophy-associated dilated cardiomyopathy: mechanisms and experimental therapeutic strategies. *J Clin Med*. 2020;9:520. doi: 10.3390/jcm9020520

9. Rossi AE, Dirksen RT. Sarcoplasmic reticulum: the dynamic calcium governor of muscle. *Muscle Nerve*. 2006;33:715–731. doi: 10.1002/mus.20512

10. Periasamy M, Kalyanasundaram A. SERCA pump isoforms: their role in calcium transport and disease. *Muscle Nerve*. 2007;35:430–442. doi: 10.1002/mus.20745

11. Xu H, Van Remmen H. The SarcoEndoplasmic Reticulum Calcium ATPase (SERCA) pump: a potential target for intervention in aging and skeletal muscle pathologies. *Skelet Muscle*. 2021;11:25. doi: 10.1186/s13395-021-00280-7

12. Kargacin ME, Kargacin GJ. The sarcoplasmic reticulum calcium pump is functionally altered in dystrophic muscle. *Biochim Biophys Acta*. 1996;1290:4–8. doi: 10.1016/0304-4165(95)00180-8

13. Bellinger AM, Reiken S, Carlson C, Mongillo M, Liu X, Rothman L, Matecki S, Lacampagne A, Marks AR. Hypernitrosylated ryanodine receptor calcium release channels are leaky in dystrophic muscle. *Nat Med*. 2009;15:325–330. doi: 10.1038/nm.1916

14. Fauconnier J, Thireau J, Reiken S, Cassan C, Richard S, Matecki S, Marks AR, Lacampagne A. Leaky RyR2 trigger ventricular arrhythmias in Duchenne muscular dystrophy. *Proc Natl Acad Sci USA*. 2010;107:1559–1564. doi: 10.1073/pnas.0908540107

15. Schneider JS, Shanmugam M, Gonzalez JP, Lopez H, Gordan R, Fraidenraich D, Babu GJ. Increased sarcolipin expression and decreased sarco(endo)plasmic reticulum Ca uptake in skeletal muscles of mouse models of Duchenne muscular dystrophy. *J Muscle Res Cell Motil*. 2013;34:349–356. doi: 10.1007/s10974-013-9350-0

16. Morine KJ, Sleeper MM, Barton ER, Sweeney HL. Overexpression of SERCA1a in the mdx diaphragm reduces susceptibility to contraction-induced damage. *Hum Gene Ther*. 2010;21:1735–1739. doi: 10.1089/hum.2010.077

17. Goonasekera SA, Lam CK, Millay DP, Sargent MA, Hajjar RJ, Kranias EG, Molkentin JD. Mitigation of muscular dystrophy in mice by SERCA overexpression in skeletal muscle. *J Clin Invest*. 2011;121:1044–1052. doi: 10.1172/JCI43844

18. Shin J-H, Bostick B, Yue Y, Hajjar R, Duan D. SERCA2a gene transfer improves electrocardiographic performance in aged mdx mice. *J Transl Med*. 2011;9:132. doi: 10.1186/1479-5876-9-132

19. Wasala NB, Yue Y, Lostal W, Wasala LP, Niranjan N, Hajjar RJ, Babu GJ, Duan D. Single SERCA2a therapy ameliorated dilated cardiomyopathy for 18 months in a mouse model of Duchenne muscular dystrophy. *Mol Ther*. 2020;28:845–854. doi: 10.1016/j.ymthe.2019.12.011

20. Voit A, Patel V, Pachon R, Shah V, Bakhutma M, Kohlbrenner E, McArdle JJ, Dell'Italia LJ, Mendell JR, Xie LH, et al. Reducing sarcolipin expression mitigates Duchenne muscular dystrophy and associated cardiomyopathy in mice. *Nat Commun*. 2017;8:1068. doi: 10.1038/s41467-017-01146-7

21. Mareedu S, Pachon R, Thilagavathi J, Fefelova N, Balakrishnan R, Niranjan N, Xie LH, Babu GJ. Sarcolipin haploinsufficiency prevents dystrophic cardiomyopathy in mdx mice. *Am J Physiol Heart Circ Physiol*. 2021;320:H200–H210. doi: 10.1152/ajpheart.00601.2020

22. Balakrishnan R, Mareedu S, Babu GJ. Reducing sarcolipin expression improves muscle metabolism in mdx mice. *Am J Physiol Cell Physiol*. 2022;322:C260–C274. doi: 10.1152/ajpcell.00125.2021

23. Nelson BR, Makarewich CA, Anderson DM, Winders BR, Troupes CD, Wu F, Reese AL, McAnally JR, Chen X, Kavalali ET, et al. A peptide

encoded by a transcript annotated as long noncoding RNA enhances SERCA activity in muscle. *Science*. 2016;351:271–275. doi: 10.1126/science.aad4076

24. Makarewich CA, Munir AZ, Schiattarella GG, Bezprozvannaya S, Raguimova ON, Cho EE, Vidal AH, Robia SL, Bassel-Duby R, Olson EN. The DWORF micropeptide enhances contractility and prevents heart failure in a mouse model of dilated cardiomyopathy. *Elife*. 2018;7:7. doi: 10.7554/eLife.38319

25. Makarewich CA, Bezprozvannaya S, Gibson AM, Bassel-Duby R, Olson EN. Gene therapy with the DWORF micropeptide attenuates cardiomyopathy in mice. *Circ Res*. 2020;127:1340–1342. doi: 10.1161/CIRCRESAHA.120.317156

26. Apkon S, Kinnett K, Cripe L, Duan D, Jackson JL, Kornegay JN, Mah ML, Nelson SF, Rao V, Scavina M, et al. Parent Project Muscular Dystrophy females with Dystrophinopathy conference, Orlando, Florida June 26–June 27, 2019. *J Neuromuscul Dis*. 2021;8:315–322. doi: 10.3233/JND-200555

27. Bostick B, Yue Y, Duan D. Gender influences cardiac function in the mdx model of Duchenne cardiomyopathy. *Muscle Nerve*. 2010;42:600–603. doi: 10.1002/mus.21763

28. Hakim CH, Duan D. Gender differences in contractile and passive properties of mdx extensor digitorum longus muscle. *Muscle Nerve*. 2012;45:250–256. doi: 10.1002/mus.22275

29. Bostick B, Yue Y, Long C, Marschalk N, Fine DM, Chen J, Duan D. Cardiac expression of a mini-dystrophin that normalizes skeletal muscle force only partially restores heart function in aged mdx mice. *Mol Ther*. 2009;17:253–261. doi: 10.1038/mt.2008.264

30. Shin J-H, Yue Y, Duan D. Recombinant adeno-associated viral vector production and purification. *Methods Mol Biol*. 2012;798:267–284. doi: 10.1007/978-1-61779-343-1_15

31. Babu GJ, Bhupathy P, Carnes CA, Billman GE, Periasamy M. Differential expression of sarcolipin protein during muscle development and cardiac pathophysiology. *J Mol Cell Cardiol*. 2007;43:215–222. doi: 10.1016/j.yjmcc.2007.05.009

32. Duan D, Rafael-Fortney JA, Blain A, Kass DA, McNally EM, Metzger JM, Spurney CF, Kinnett K. Standard operating procedures (SOPs) for evaluating the heart in preclinical studies of Duchenne muscular dystrophy. *J Cardiovasc Transl Res*. 2016;9:85–86. doi: 10.1007/s12265-015-9669-6

33. Mitchell GF, Jeron A, Koren G. Measurement of heart rate and Q-T interval in the conscious mouse. *Am J Physiol*. 1998;274:H747–H751. doi: 10.1152/ajpheart.1998.274.3.H747

34. Bostick B, Yue Y, Duan D. Phenotyping cardiac gene therapy in mice. *Methods Mol Biol*. 2011;709:91–104. doi: 10.1007/978-1-61737-982-6_6

35. Weiss JL, Frederiksen JW, Weisfeldt ML. Hemodynamic determinants of the time-course of fall in canine left ventricular pressure. *J Clin Invest*. 1976;58:751–760. doi: 10.1172/JCI108522

36. Cheung MC, Spalding PB, Gutierrez JC, Balkan W, Namias N, Koniaris LG, Zimmers TA. Body surface area prediction in normal, hypermuscular, and obese mice. *J Surg Res*. 2009;153:326–331. doi: 10.1016/j.jss.2008.05.002

37. Bostick B, Ghosh A, Yue Y, Long C, Duan D. Systemic AAV-9 transduction in mice is influenced by animal age but not by the route of administration. *Gene Ther*. 2007;14:1605–1609. doi: 10.1038/sj.gt.3303029

38. Bostick B, Yue Y, Long C, Duan D. Prevention of dystrophin-deficient cardiomyopathy in twenty-one-month-old carrier mice by mosaic dystrophin expression or complementary dystrophin/utrophin expression. *Circ Res*. 2008;102:121–130. doi: 10.1161/CIRCRESAHA.107.162982

39. Bernstein D. Exercise assessment of transgenic models of human cardiovascular disease. *Physiol Genomics*. 2003;13:217–226. doi: 10.1152/physiolgenomics.00188.2002

40. Singh DR, Dalton MP, Cho EE, Pribadi MP, Zak TJ, Seflova J, Makarewich CA, Olson EN, Robia SL. Newly discovered micropeptide regulators of SERCA form oligomers but bind to the pump as monomers. *J Mol Biol*. 2019;431:4429–4443. doi: 10.1016/j.jmb.2019.07.037

41. Fisher ME, Bovo E, Aguayo-Ortiz R, Cho EE, Pribadi MP, Dalton MP, Rathod N, Lemieux MJ, Espinoza-Fonseca LM, Robia SL, et al. Dwarf open reading frame (DWORF) is a direct activator of the sarcoplasmic reticulum calcium pump SERCA. *Elife*. 2021;10:10. doi: 10.7554/eLife.65545

42. Reddy UV, Weber DK, Wang S, Larsen EK, Gopinath T, De Simone A, Robia S, Veglia G. A kink in DWORF helical structure controls the activation of the sarcoplasmic reticulum Ca(2+)-ATPase. *Structure*. 2022;30:360–370.e6. doi: 10.1016/j.str.2021.11.003

43. Li A, Yuen SL, Stroik DR, Kleinboehl E, Cornea RL, Thomas DD. The transmembrane peptide DWORF activates SERCA2a via dual mechanisms. *J Biol Chem*. 2021;296:100412. doi: 10.1016/j.jbc.2021.100412

44. Niranjan N, Mareedu S, Tian Y, Kodippili K, Fefelova N, Voit A, Xie LH, Duan D, Babu GJ. Sarcolipin overexpression impairs myogenic differentiation in Duchenne muscular dystrophy. *Am J Physiol Cell Physiol*. 2019;317:C813–C824. doi: 10.1152/ajpcell.00146.2019

45. Duan D. Challenges and opportunities in dystrophin-deficient cardiomyopathy gene therapy. *Hum Mol Genet*. 2006;15:R253–R261. doi: 10.1093/hmg/ddl180

46. Srivastava A. AAV vectors: are they safe? *Hum Gene Ther*. 2020;31:697–699. doi: 10.1089/hum.2020.187

47. Mbikou P, Rademaker MT, Charles CJ, Richards MA, Pemberton CJ. Cardiovascular effects of DWORF (dwarf open reading frame) peptide in normal and ischaemia/reperfused isolated rat hearts. *Peptides*. 2020;124:170192. doi: 10.1016/j.peptides.2019.170192

48. Law ML, Prins KW, Olander ME, Metzger JM. Exacerbation of dystrophic cardiomyopathy by phospholamban deficiency mediated chronically increased cardiac Ca(2+) cycling in vivo. *Am J Physiol Heart Circ Physiol*. 2018;315:H1544–H1552. doi: 10.1152/ajpheart.00341.2018

49. Fajardo VA, Chambers PJ, Juracic ES, Rietze BA, Gamu D, Bellissimo C, Kwon F, Quadrilatero J, Russell Tupling A. Sarcolipin deletion in mdx mice impairs calcineurin signalling and worsens dystrophic pathology. *Hum Mol Genet*. 2018;27:4094–4102. doi: 10.1093/hmg/ddy302

50. Duan D. Micro-dystrophin gene therapy goes systemic in Duchenne muscular dystrophy patients. *Hum Gene Ther*. 2018;29:733–736. doi: 10.1089/hum.2018.012

51. Shin J-H, Pan X, Hakim CH, Yang HT, Yue Y, Zhang K, Terjung RL, Duan D. Microdystrophin ameliorates muscular dystrophy in the canine model of Duchenne muscular dystrophy. *Mol Ther*. 2013;21:750–757. doi: 10.1038/mt.2012.283

52. Mullard A. Sarepta's DMD gene therapy falls flat. *Nat Rev Drug Discov*. 2021;20:91. doi: 10.1038/d41573-021-00010-0

SUPPLEMENTAL MATERIAL

Table S1. Left ventricle hemodynamic parameters.

	Wild type	mdx	mdx AAV.DWORF
Sample Size (N)	23	20	9
Body Surface Area (cm^2)	93.50 ± 1.91 [*,§]	79.77 ± 1.06 [‖]	77.67 ± 1.68
Stroke Volume Index (mL/m^2)	1.51 ± 0.13 [§]	1.34 ± 0.10 [‖]	1.38 ± 0.17
Cardiac Index (L/min/m^2)	0.86 ± 0.09 [§]	0.72 ± 0.06 [‖]	0.72 ± 0.11
Min P (mmHg)	2.32 ± 0.62	3.15 ± 0.79	6.30 ± 2.37
End Systolic Pressure (mmHg)	89.07 ± 1.39	70.32 ± 5.19 [†]	86.53 ± 6.44
End Diastolic Pressure (mmHg)	5.08 ± 0.77	5.79 ± 1.00	8.97 ± 2.32
Stroke Work (KmmHgµL)	1118.04 ± 101.51	591.70 ± 62.28 [†]	780.78 ± 156.62
Arterial Elastance (mmHg/µL)	6.78 ± 0.52	6.78 ± 0.63	8.76 ± 1.01
dV/dt Max (µL/sec)	671.83 ± 59.21	631.30 ± 51.08	422.60 ± 35.78 [†]
dV/dt Min (µL/sec)	-779.91 ± 62.33	-708.40 ± 59.42	-582.00 ± 76.95
P@dV/dt Max (mmHg)	26.01 ± 4.97	20.91 ± 4.43	24.26 ± 9.05
P@dP/dt Max (mmHg)	60.11 ± 1.30	41.51 ± 3.74 [*]	62.52 ± 4.77 [‡]
V@dP/dt Max (µL)	21.88 ± 1.27	26.83 ± 1.73 [*]	14.60 ± 1.50 [‡]
V@dP/dt Min (µL)	8.84 ± 0.89	17.55 ± 1.59 [*]	4.96 ± 1.19 [‡]
Max Power (mWatts)	6.54 ± 0.66 [#]	5.06 ± 0.64 [**]	6.41 ± 1.31
Preload Adjusted Max Power (mWatts/µL^2)	244.42 ± 37.59 [#]	145.85 ± 26.04 [**]	463.44 ± 132.01 [‡]

(left margin label for above section: Mean ± Standard error of mean)

	Wild type	mdx	mdx AAV.DWORF
Body Surface Area (cm^2)	92.50 (89.00, 97.00)	80.00 (77.75, 80.75)	79.00 (76.00, 80.50)
Stroke Volume Index (mL/m^2)	1.38 (0.99, 1.93)	1.25 (1.08, 1.55)	1.14 (1.10, 1.55)
Cardiac Index (L/min/m^2)	0.74 (0.57, 1.23)	0.71 (0.54, 0.85)	0.58 (0.53, 0.83)
Min P (mmHg)	1.38 (0.67, 2.98)	2.05 (1.11, 4.12)	1.63 (1.27, 10.50)
End Systolic Pressure (mmHg)	88.73 (84.14, 94.37)	74.75 (52.97, 81.55)	96.67 (70.09, 100.30)
End Diastolic Pressure (mmHg)	3.60 (2.80, 6.12)	4.23 (2.86, 7.46)	5.53 (3.66, 12.59)
Stroke Work (KmmHgµL)	1026.00 (729.75, 1592.25)	600.00 (451.50, 720.00)	625.00 (483.25, 827.50)

(left margin label for above section: 75th percentile)

	Arterial Elastance (mmHg/µL)	6.50 (4.57, 8.82)	6.64 (4.37, 9.15)	9.47 (6.40, 10.21)
	dV/dt Max (µL/sec)	621.00 (470.75, 773.00)	595.50 (425.00, 832.50)	384.50 (326.00, 516.00)
	dV/dt Min (µL/sec)	-757.00 (-983.75, -503.25)	-686.00 (-851.50, -493.00)	-513.00 (-655.50, -428.75)
	P@dV/dt Max (mmHg)	21.17 (4.25, 48.36)	16.32 (3.57, 32.71)	15.52 (4.87, 34.34)
Median (25th percentile,	P@dP/dt Max (mmHg)	58.83 (55.82, 63.09)	41.82 (30.71, 51.87)	69.99 (49.60, 74.64)
	V@dP/dt Max (µL)	22.12 (18.18, 24.41)	27.57 (20.18, 31.97)	11.94 (11.23, 19.09)
	V@dP/dt Min (µL)	8.49 (4.94, 11.61)	17.70 (12.79, 22.59)	3.71 (2.79, 5.48)
	Max Power (mWatts)	5.79 (4.71, 8.80)	4.39 (4.07, 5.69)	5.97 (3.47, 8.06)
	Preload Adjusted Max Power (mWatts/µL^2)	221.56 (143.52, 326.78)	144.70 (90.05, 161.18)	313.87 (192.14, 602.61)

*, significantly different from other two groups

†, significantly different from WT

‡, significantly different from mdx

§, N=18; ‖, N=13; #, N=14; **, N=9

Figure S1. Uncropped western blot images from WT, mdx, and treated mdx hearts.
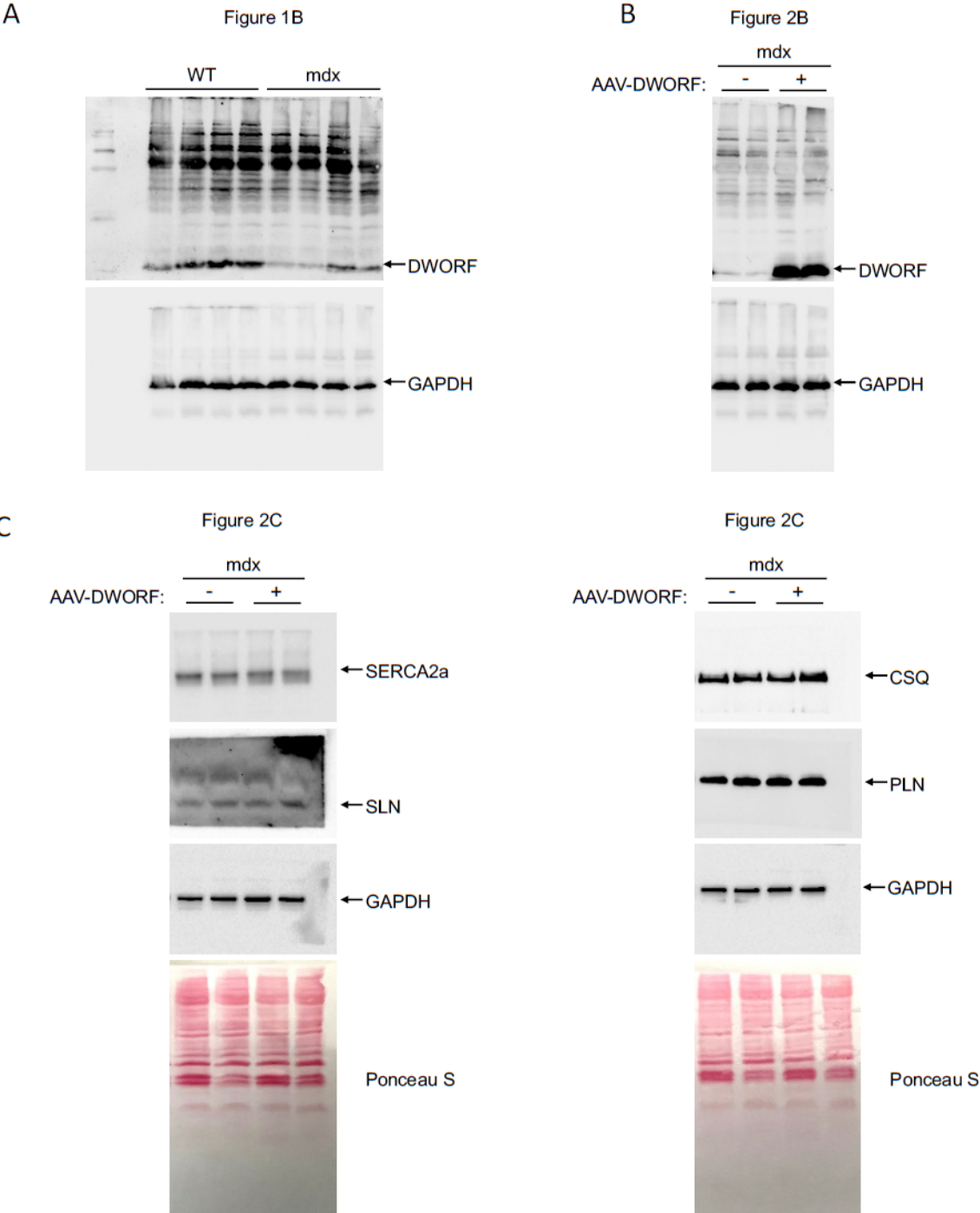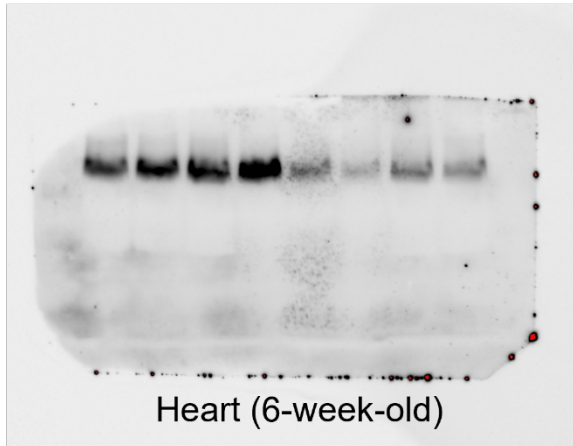

A. Uncropped western blot image for Figure 1B. **B.** Uncropped western blot image for Figure 2B. **C.** Uncropped western blot image for Figure 2C.

Figure S2. DWORF expression was reduced in the ventricles of mdx mice irrespective of age.
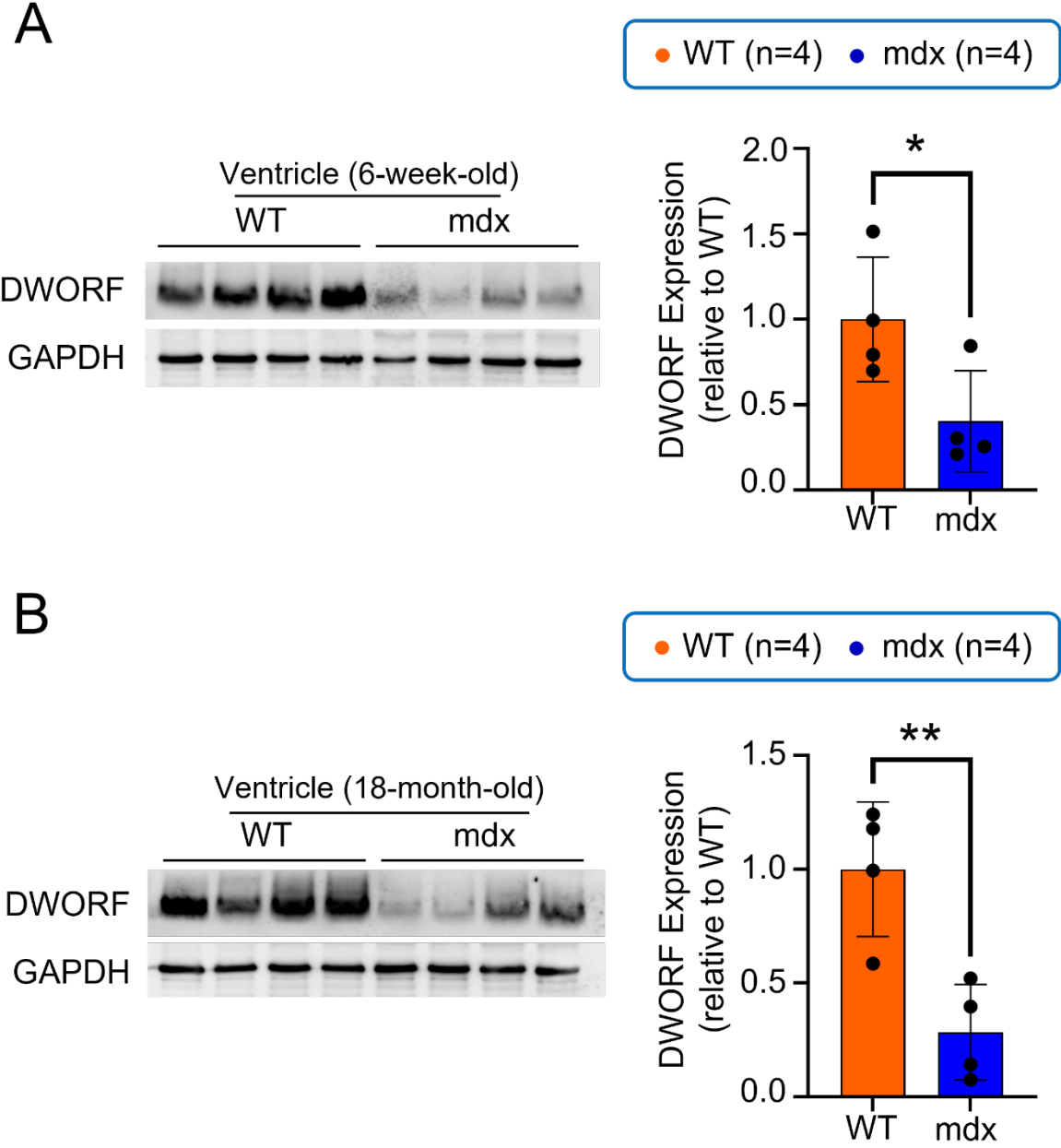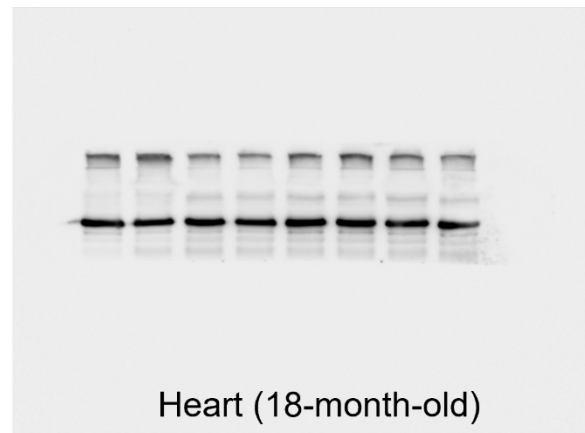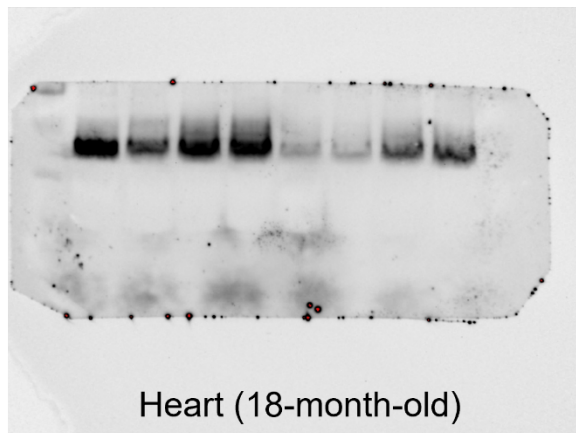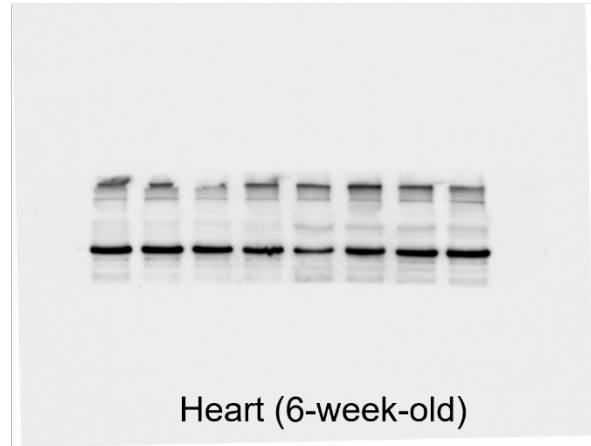
C

DWORF Western	GAPDH Western

Heart (6-week-old)

Heart (6-week-old)

Heart (18-month-old)

Heart (18-month-old)

A. Quantification of DWORF protein expression in the ventricles of 6-week-old WT and mdx mice by western blot. The left panel shows western blot images, and the right panel shows densitometry results. **B.** Quantification of DWORF protein expression in the ventricles of 18-month-old WT and mdx mice by western blot. The left panel shows western blot images, and the right panel shows densitometry results. **C.** Uncropped western blot image for panels A and B. Sample size refers to the number of mice used in the study. Data are presented as mean ± S.E.M. *p<0.05; **p<0.01; **p<0.001.

Figure S3. Unexpected observation of protein expression from the internal ribosomal entry site (IRES) used in the study.
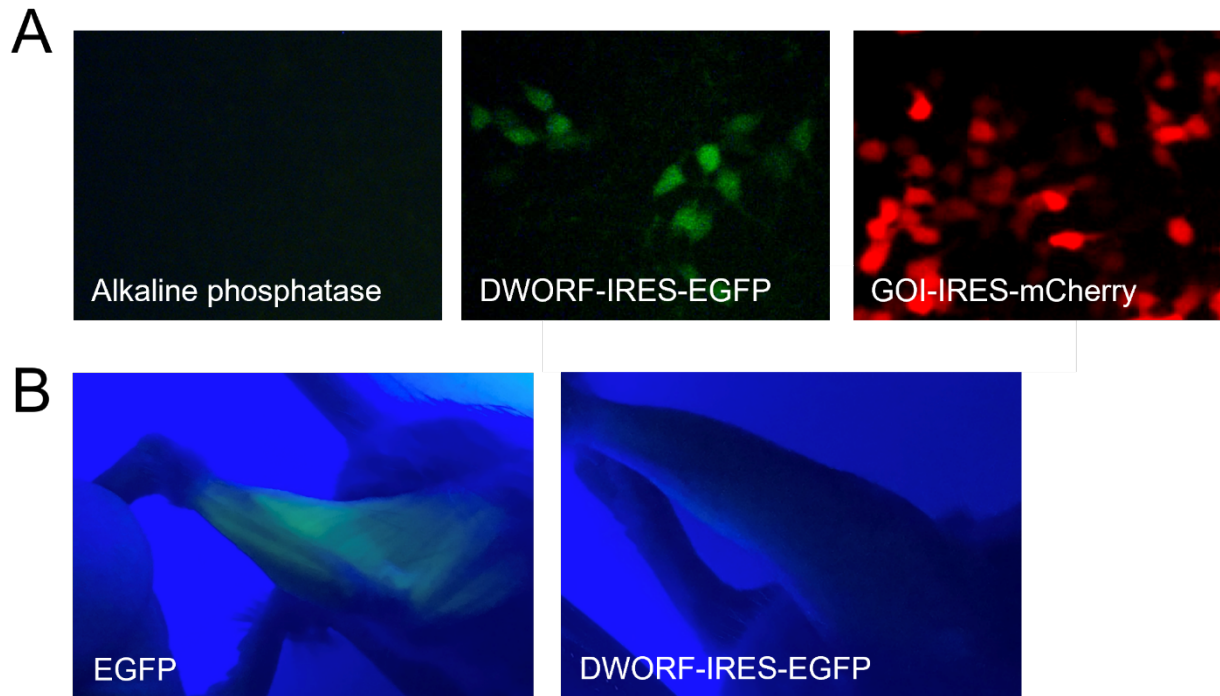

A. IRES resulted in efficient transgene expression in 293 cells. Three independent plasmids were used in transfection. One plasmid expressed non-fluorescent reporter alkaline phosphatase from the RSV promoter (left panel). The second plasmid (the plasmid used in the current study) expressed EGFP from the IRES (middle panel). The third plasmid expressed mCherry from the IRES (right panel). GOI, gene of interest. **B.** IRES failed to mediate EGFP expression in mouse muscle in vivo. EGFP expression was readily visualized in leg muscles 4 weeks following systemic injection of an AAV9.CMV.EGFP vector (6 x 10^{12} vg particles/mouse) in 6-week-old mdx mice (left panel). EGFP expression was not detected in leg muscles 4 weeks following systemic injection of the AAV9.CAG.DWORF-IRES-EGFP vector (6 x 10^{12} vg particles/mouse) in 6-week-old mdx mice (right panel).

Figure S4. AAV-mediated DWORF expression did not alter the level of the endogenous DWORF transcripts.
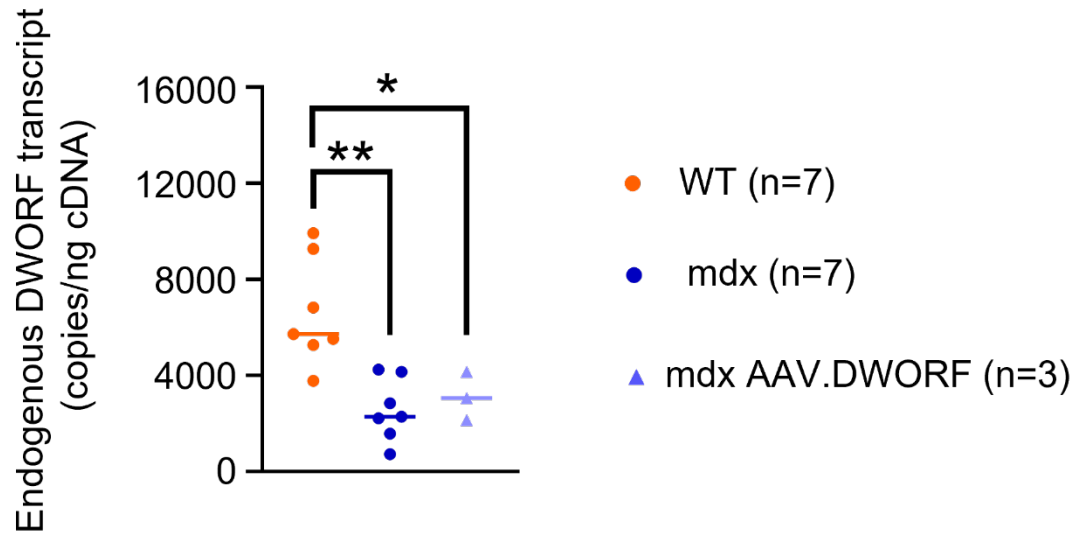

Quantification of endogenous DWORF transcript by digital droplet PCR. Sample size refers to the number of mice used in the study. Data are presented as mean ± S.E.M. *p<0.05; **p<0.01.

Figure S5. Box plot presentations of ECG data analyzed by Kruskal-Wallis test.
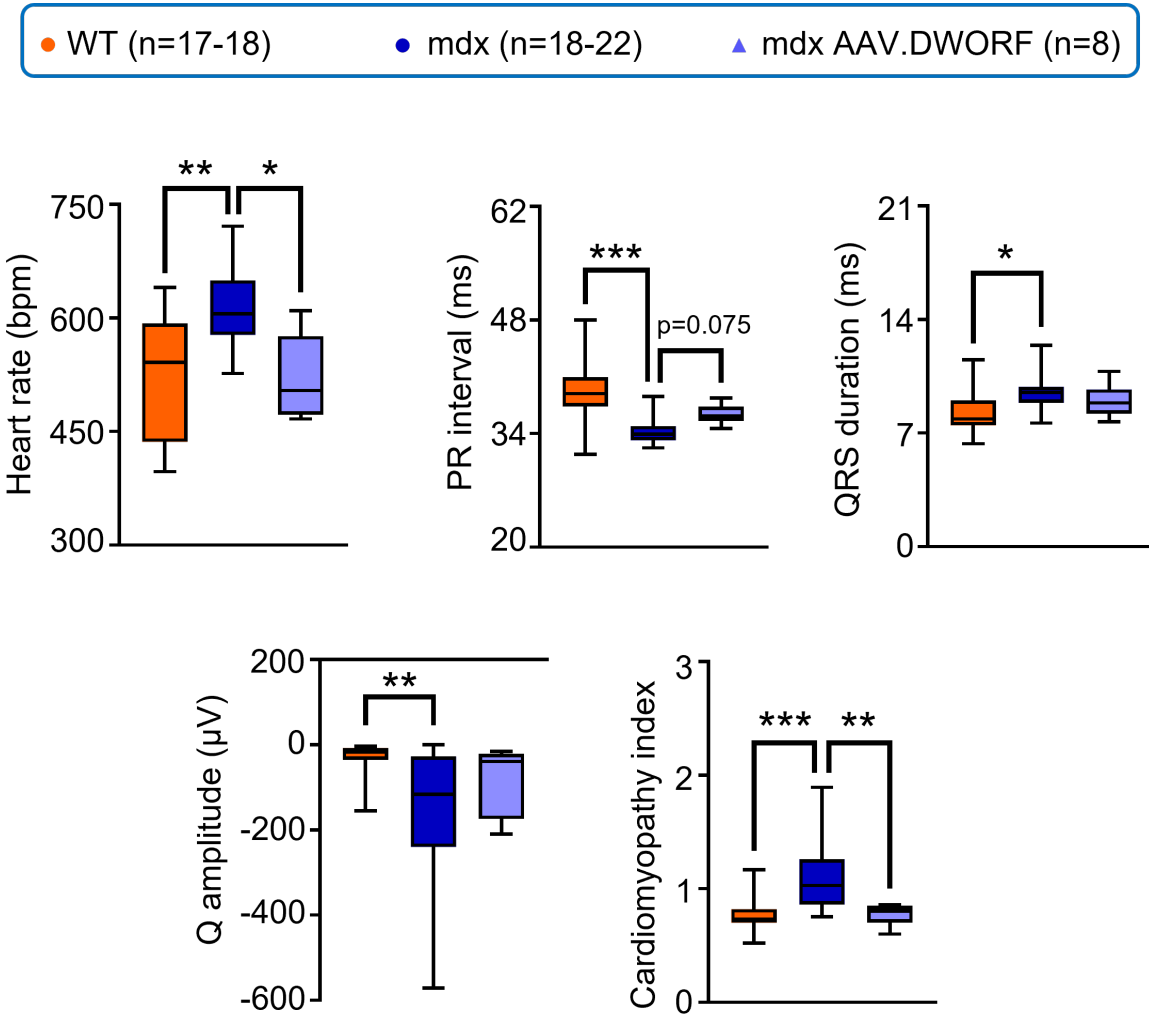

The bottom and top of the box are the 25th (quartile 1, Q1) and 75th percentiles (Q3). The line inside the box is the 50th percentile (median). Whiskers are 1.5 times the interquartile range beyond Q1 and Q3. *, $p < 0.05$; **, $p < 0.01$; ***, $p < 0.001$.

Figure S6. Box plot presentations of hemodynamic data analyzed by Kruskal-Wallis test.
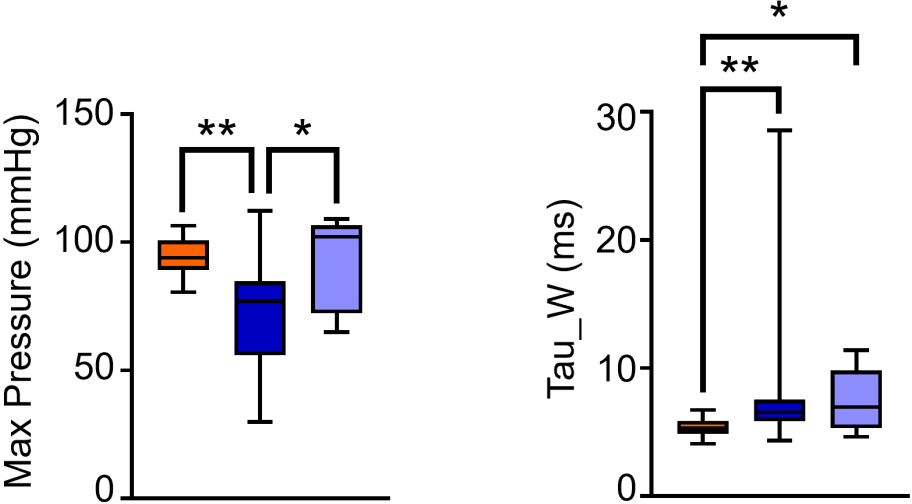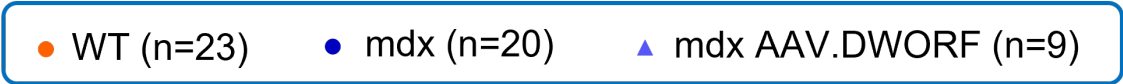
The bottom and top of the box are the 25th (quartile 1, Q1) and 75th percentiles (Q3). The line inside the box is the 50th percentile (median). Whiskers are 1.5 times the interquartile range beyond Q1 and Q3. *, $p < 0.05$; **, $p < 0.01$.
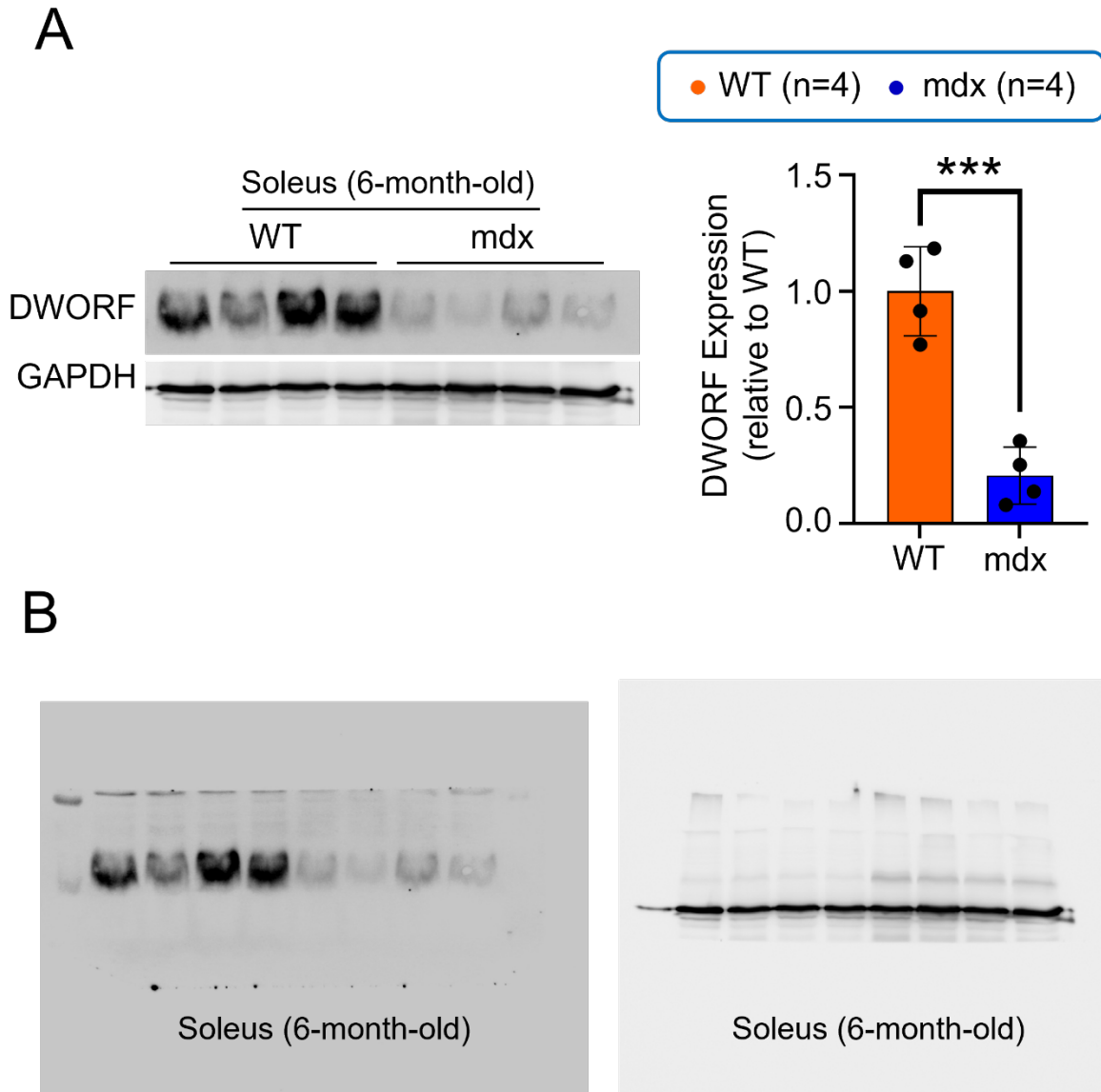
Figure S7. Pressure-volume (PV) loops of AAV DWORF-treated mdx mice.
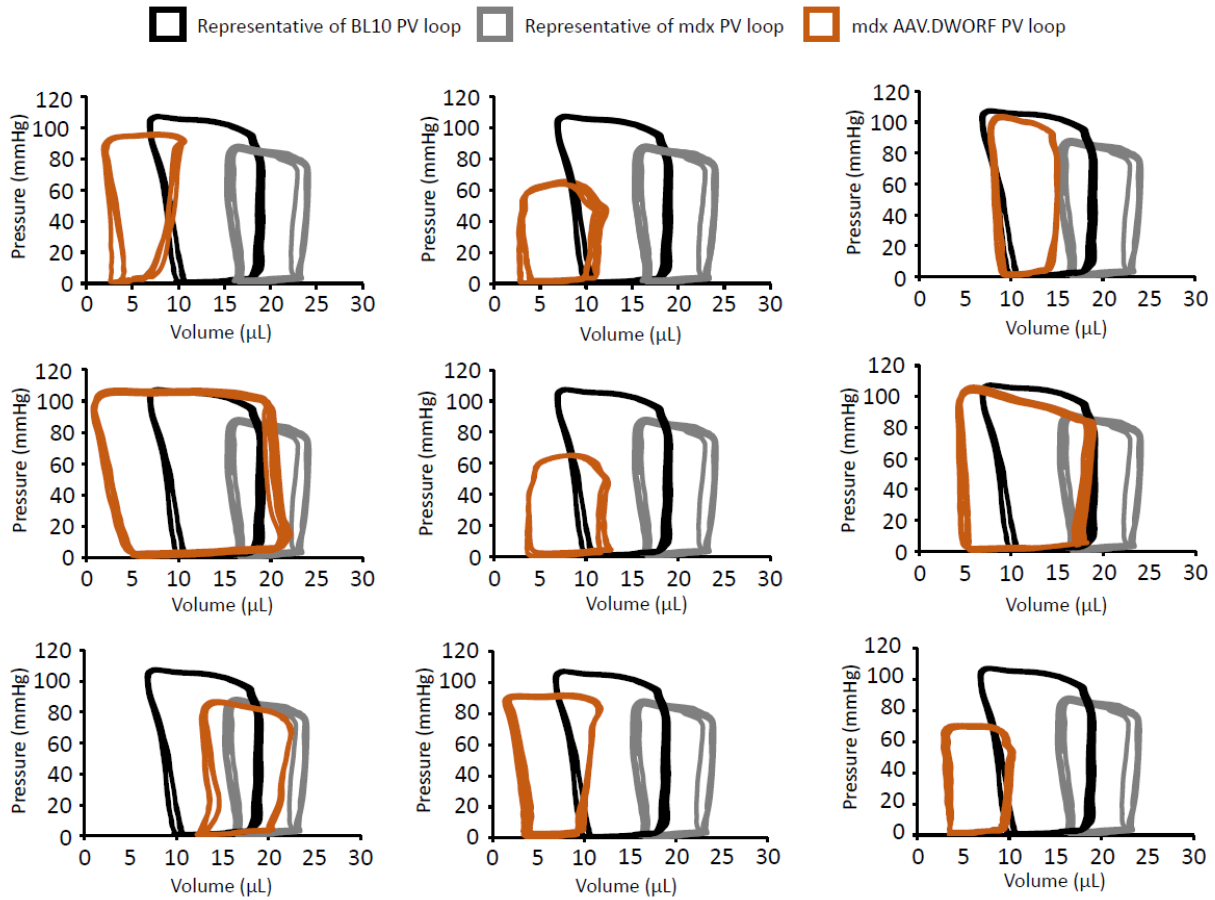
PV loops of AAV.DWORF-treated mdx mice are shown on the background of representative PV loops from a wild-type mouse and an mdx mouse. The top left panel is shown in Figure 6 of the main article.

Figure S8. DWORF expression was reduced in the soleus muscle of mdx.

A

B

A. Quantification of DWORF protein expression in the soleus of 6-month-old wild-type and mdx mice by western blot. The left panel shows western blot images, and the right panel shows densitometry results. **B.** Uncropped western blot image for panel A. Sample size refers to the number of mice used in the study. Data are presented as mean ± S.E.M. *p<0.001.